NUMERICAL ANALYSIS OF FINITE AXISYMMETRIC DEFORMATIONS OF INCOMPRESSIBLE ELASTIC SOLIDS OF REVOLUTION

J. T. ODEN† and J. E. KEY‡

Research Institute, University of Alabama in Huntsville, Alabama.

Abstract—This paper is concerned with the application of the finite element method to the problem of finite axisymmetric deformations of incompressible, elastic solids of revolution. On the basis of approximate displacement fields, nonlinear stiffness relations are derived for a typical finite element. These relations involve an additional unknown, the hydrostatic pressure, which necessitates the introduction of an incompressibility condition for each element. Provisions are also made to account for changes in loading due to deformation. A brief discussion of several methods used for solving the systems of nonlinear equations generated in the analysis is also given. Numerical solutions to representative problems are included.

1. INTRODUCTION

RELATIVELY few exact solutions to problems of finite axisymmetric deformations of elastic solids of revolution are available in the literature, and all appear to deal with bodies of the most simple geometric shapes, and to be based on the assumption that the deformed shape of the body, equally simple in geometry, is also specified *a priori*. For example, the problem of symmetric deformations of a tube subjected to uniform external and internal pressure is included as a special case of a problem solved by Rivlin [1]; Ericksen and Rivlin [2] considered the simultaneous inflation and elongation of a hollow cylinder; Rivlin and Thomas [3] examined radial deformations of a thin sheet containing a circular hole; and Green and Shield [4] investigated symmetrical expansions of a spherical shell. Summary accounts of solutions to related problems in finite elasticity can be found in the books of Green and Zerna [5], Green and Adkins [6], Truesdell and Noll [7], Eringen [8], and in the collection of reprinted articles edited by Truesdell [9]. More recently, Baltrukonis and Vaishnav [10] presented solutions to the problem of axisymmetric deformations of an infinite hollow elastic cylinder bonded to a thin elastic case. As indicated by Green and Shield [4], it does not appear to be possible to obtain exact solutions to the more general problem of finite axisymmetric deformations owing to the nonlinearity of the governing differential equations and the complexities inherent in irregular geometries and boundary conditions. Thus, it is natural to seek approximate solutions to this class of problems.

In the present paper, we consider the general problem of finite axisymmetric deformations of incompressible elastic solids of revolution of arbitrary cross-sectional shape subjected to general axisymmetric loading and boundary conditions. We formulate solutions of this problem in terms of generalizations of the finite-element technique.

† Professor of Engineering Mechanics.
‡ Graduate Student, Division of Engineering.

On the basis of approximations to the displacement fields over finite elements of revolution, we derive nonlinear stiffness relations for typical finite elements and use these relations to solve representative problems in finite elasticity.

Applications of the finite-element method to the linear problem of symmetric infinitesimal deformations of Hookean solids of revolution were recently given by Rashid [11], Clough and Rashid [12], and Rashid [13]. Wilson [14] considered the linear problem of general, infinitesimal deformations of axisymmetric elastic solids and Becker and Brisbane [15], using the variational theorem of Herrmann [16], developed finite element models for the analysis of infinitesimal axisymmetric deformations of incompressible elastic solids of revolution. Extensions of the method to finite elasticity problems have been given by Oden [17–19], Oden and Sato [20, 21], Oden and Kubitza [22], Becker [23], and for a class of plane stress problems involving large strains by Herrmann [24], Peterson, Campbell, and Herrmann [25], and moderately large strains by Argyris [26]. A survey of literature on applications of this and related numerical techniques to problems of solid propellants has been given by Parr [27].

In this paper, we present, in the section following this introduction, a brief review of the basic equations of the theory of finite deformations of elastic solids of revolution. In Section 3 we discuss the finite-element representation of displacement fields of arbitrary solids, and in the next section we bring these ideas together to obtain nonlinear stiffness relations for typical finite elements. For incompressible finite elements, these relations involve an unknown hydrostatic pressure corresponding to each element, and it is necessary to introduce a supplementary condition of incompressibility for each finite element. We then pay special attention to forms of the equations corresponding to Mooney-type materials, for these lead to results which can be compared to exact solutions already available. In Section 5 we briefly examine several numerical methods for solving the large systems of nonlinear equations generated in the analysis. We then present numerical solutions to representative problems, including the problem of finite deformation of an incompressible hollow cylinder.

2. FINITE AXISYMMETRIC DEFORMATIONS

We briefly examine here several relations drawn from the theory of finite elasticity [5, 6]. We consider an elastic solid of revolution of arbitrary cross-sectional shape and suppose that the locations of material particles in a reference configuration of the body are given by the convected (intrinsic) cylindrical coordinates $x^1 = r$, $x^2 = z$ and $x^3 = \theta$. The deformation of the body is determined by the displacement field $\mathbf{u} = \mathbf{u}(r, z, \theta)$ and its gradient $\mathbf{u}_{,i} \equiv \partial \mathbf{u}/\partial x^i$.

In the following, we confine our attention to the case of purely axisymmetric deformations, for which $\mathbf{u} = \mathbf{u}(r, z)$ and the displacement field is determined by radial and axial components, u_1 and u_2. In this case, the strain–displacement relations reduce to

$$
\left.
\begin{aligned}
2\gamma_{\alpha\beta} &= u_{\alpha,\beta} + u_{\beta,\alpha} + u_{\mu,\alpha} u^{\mu}_{,\beta} \\[2mm]
\gamma_{\alpha 3} &= 0 \\[2mm]
\gamma_{33} &= \frac{r^2}{2}(\lambda^2 - 1)
\end{aligned}
\right\}
\tag{1}
$$

where $\gamma_{\alpha\beta}(\alpha, \beta, \mu = 1, 2)$ are the covariant components of the strain tensor, $u_\mu = u^\mu$ and

$$\lambda = 1 + \frac{u_1}{r}. \tag{2}$$

The function $\lambda = \lambda(r, z)$ is the extension ratio in the circumferential direction; that is, λ is the ratio of the length of a circumferential fiber in the deformed body to its original length in the reference configuration.

We assume that the material is characterized by a potential function $W = \overline{W}(\gamma_{ij})$ which represents the strain energy per unit volume in the undeformed body. The stress tensor σ^{ij} referred to the convected coordinates x^i in the deformed body is then given by [5]

$$\sigma^{ij} = \frac{1}{2}\sqrt{\left(\frac{g}{G}\right)}\left(\frac{\partial \overline{W}}{\partial \gamma_{ij}} + \frac{\partial \overline{W}}{\partial \gamma_{ji}}\right) \tag{3}$$

where g and G denote the determinant of the metric tensors, g_{ij} and G_{ij}, in the undeformed and deformed body, respectively. For an isotropic body, the strain energy function can be written

$$W = \overline{W}(I_1, I_2, I_3) \tag{4}$$

where I_1, I_2, I_3 are principal invariants of the deformation tensor. For the type of deformations under consideration,

$$\left.\begin{aligned} I_1 &= 2(1 + \gamma_\alpha^\alpha) + \lambda^2 \\ I_2 &= 2\lambda^2(1 + \gamma_\alpha^\alpha) + \varphi \\ I_3 &= \lambda^2 \varphi \end{aligned}\right\} \tag{5}$$

where

$$\varphi = 1 + 2\gamma_\alpha^\alpha + 2\,e^{\alpha\beta}\,e^{\lambda\mu}\gamma_{\alpha\lambda}\gamma_{\beta\mu} \tag{6}$$

and $e^{\alpha\beta}$ is the two-dimensional permutation symbol ($e^{12} = -e^{21} = 1; e^{11} = e^{22} = 0$).

In the case of incompressible, isotropic elastic solids, $I_3 = 1$, $W = \hat{W}(I_1, I_2)$ and the strain energy determines the stress only to within an arbitrary hydrostatic pressure h. Then (3) reduces to

$$\sigma^{ij} = \frac{1}{2}\left\{\frac{\partial \hat{W}}{\partial I_1}\left(\frac{\partial I_1}{\partial \gamma_{ij}} + \frac{\partial I_1}{\partial \gamma_{ji}}\right) + \frac{\partial \hat{W}}{\partial I_2}\left(\frac{\partial I_2}{\partial \gamma_{ij}} + \frac{\partial I_2}{\partial \gamma_{ji}}\right)\right\} + \frac{1}{2}h\left(\frac{\partial I_3}{\partial \gamma_{ij}} + \frac{\partial I_3}{\partial \gamma_{ji}}\right). \tag{7}$$

For axisymmetric deformations of incompressible, isotropic solids of revolution, (7) yields

$$\left.\begin{aligned} \sigma^{\alpha\beta} &= 2\frac{\partial \hat{W}}{\partial I_1}\delta^{\alpha\beta} + 2\frac{\partial \hat{W}}{\partial I_2}[\delta^{\alpha\beta}(1 + \lambda^2) + 2e^{\alpha\lambda}\,e^{\beta\mu}\gamma_{\lambda\mu}] + 2h\lambda^2(\delta^{\alpha\beta} + 2e^{\alpha\lambda}\,e^{\beta\mu}\gamma_{\lambda\mu}) \\ \sigma^{\alpha 3} &= 0 \\ r^2\sigma^{33} &= 2\frac{\partial \hat{W}}{\partial I_1} + 4(1 + \gamma_\alpha^\alpha)\frac{\partial \hat{W}}{\partial I_2} + 2h\varphi \end{aligned}\right\}. \tag{8}$$

3. FINITE ELEMENT APPROXIMATION

We now set out to construct a discrete model of the body by representing it as a collection of a number E of finite elements of revolution, as indicated in Fig. 1. Following the usual procedure, we isolate a typical finite element e and approximate the local displacement field $u_\alpha(x^1, x^2)$ over the element by functions of the form [28–31]
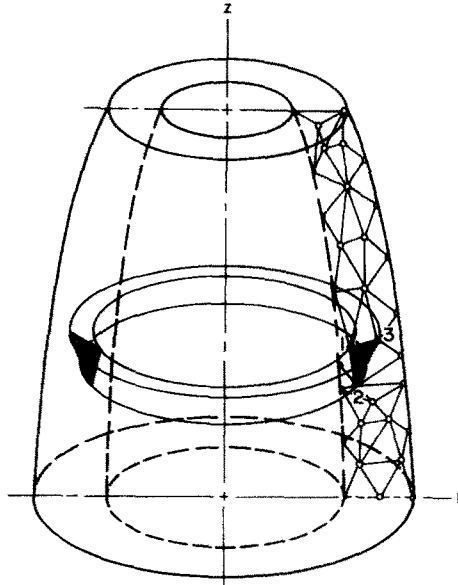
$$u_\alpha = \Psi^N(\mathbf{x})u_{N\alpha} \tag{9}$$

FIG. 1. Finite-element model of a solid of revolution.

where $\mathbf{x} = (x^1, x^2)$ and $u_{N\alpha}$ are the components of displacement of node N of the element and $\Psi^N(\mathbf{x})$ are interpolation functions with the property

$$\Psi^N(\mathbf{x}_M) = \delta_M^N \tag{10}$$

in which $\mathbf{x}_M = x_M^\beta$ are the local coordinates of node M and δ_M^N is the Kronecker delta. In (9) and in developments to follow, the repeated nodal index N is to be summed from 1 to N_e, N_e being the total number of node points belonging to element e.

In the present study we shall give special attention to simple triangular elements $(N_e = 3)$, in which case [18, 19, 29]

$$\Psi^N(x^1, x^2) = a^N + b_\beta^N x^\beta \tag{11}$$

in which

$$a^N = \frac{1}{4A_0} e^{NMK} e_{\lambda\mu} x_M^\lambda x_K^\mu \tag{12}$$

and

$$b^N_{\cdot\beta} = \frac{1}{2A_0} \begin{bmatrix} x^2_2 - x^2_3 & x^1_3 - x^1_2 \\ \hline x^2_3 - x^2_1 & x^1_1 - x^1_3 \\ \hline x^2_1 - x^2_2 & x^1_2 - x^1_1 \end{bmatrix}. \tag{13}$$

Here e^{NMK} is the three-dimensional permutation symbol, $e_{\lambda\mu} = e^{\lambda\mu}$, A_0 is the undeformed triangular area (assuming a counter-clockwise numbering of nodes as indicated in Fig. 1), and, as noted previously, $x^\lambda_M (M = 1, 2, 3; \lambda = 1, 2)$ are the coordinates of node M. In this case, (9) assumes the simple linear form

$$u_\alpha = a^N u_{N\alpha} + b^N_{\cdot\beta} u_{N\alpha} x^\beta \tag{14}$$

Introducing (14) into (1), we find that for the finite element

$$\left. \begin{aligned} 2\gamma_{\alpha\beta} &= b^N_{\cdot\beta} u_{N\alpha} + b^N_{\cdot\alpha} u_{N\beta} + b^M_{\cdot\alpha} b^N_{\cdot\beta} u_{M\mu} u^\mu_N \\ 2\gamma_{33} &= r^2(\lambda^2 - 1) \\ \lambda &= 1 + \frac{1}{r}(a^N u_{N1} + b^N_{\cdot\beta} u_{N1} x^\beta) \end{aligned} \right\} \tag{15}$$

with $x^1 \equiv r$ and $u_{M\mu} = u^\mu_M$. Stresses in the element can be obtained by introducing (15) into (8) once the appropriate form of $\hat{W}$ has been identified.

4. NONLINEAR STIFFNESS RELATIONS

We now isolate a typical finite element and, following the same scheme outlined in previous work [18, 19], introduce the potential energy functional

$$V(\mathbf{u}) = \int_{v_0} \overline{W} \, dv - \int_{v_0} F^\alpha u_\alpha \, dv - \int_{S_0} S^\alpha u_\alpha \, dS \tag{16}$$

in which F^α and S^α are the components of body force per unit of undeformed volume v_0 and surface traction per unit undeformed area S_0, respectively. By introducing (9) into (16) and using the principle of minimum potential energy, we obtain the nonlinear stiffness relations

$$\frac{\partial V(\mathbf{u})}{\partial u_{N\alpha}} = 0 = \int_{v_0} \frac{\partial \overline{W}}{\partial \gamma_{ij}} \frac{\partial \gamma_{ij}}{\partial u_{N\alpha}} \, dv - p^{N\alpha} \tag{17}$$

where $p^{N\alpha}$ are the components of generalized force at node N:

$$p^{N\alpha} = \int_{v_0} \Psi^N(\mathbf{x}) F^\alpha \, dv + \int_{S_0} \Psi^N(\mathbf{x}) S^\alpha \, dS. \tag{18}$$

The fact that the tractions S^α also depend on the displacements $u_{N\alpha}$ is examined later.

In the present analysis, however, we are particularly interested in finite deformations of incompressible, isotropic elastic solids. Then the strain energy function is of the form $W = \hat{W}(I_1, I_2)$ and the volume of the element is conserved during the deformation. Since

the local incompressibility condition, $I_3 = 1$, is to hold at every point in the continuum, we require that for the finite element

$$\int_{v_0} (I_3 - 1)\,\mathrm{d}v = 0. \tag{19}$$

Alternately, we can obtain an equivalent incompressibility condition by simply comparing the volume v_0 and v of the element in the undeformed and deformed body:

$$H(u_{N\alpha}) \equiv v(u_{N\alpha}) - v_0 = 0 \tag{20}$$

in which

$$v_0 = 2\pi \bar{r} A_0 \qquad\qquad v = 2\pi(\bar{r} + \bar{u}_1)A \tag{21a, b}$$

$$\bar{r} = \tfrac{1}{3}(r_1 + r_2 + r_3) \qquad \bar{u}_1 = \tfrac{1}{3}(u_{11} + u_{21} + u_{31}) \tag{21c, d}$$

$$A_1 = \left| \frac{1}{2} \sum_{P=1}^{3} e^{MNP} e_{\alpha\beta 3} x_M^\alpha x_N^\beta \right| \tag{21e}$$

$$A = \left| \frac{1}{2} \sum_{P=1}^{3} e^{MNP} e_{\alpha\beta 3}(x_M^\alpha + u_M^\alpha)(x_N^\beta + u_N^\beta) \right|. \tag{21f}$$

Here $\bar{r}$ is the radial distance to the centroid of the undeformed triangular (cross-sectional) area A_0 of the element, $\bar{u}_1$ is the average of the radial displacements of nodes 1, 2 and 3 of the element, and A is the cross-sectional area of the element after deformation. Either incompressibility condition, (19) or (20), can be used, but the form of (19) is more convenient to use in deriving stiffness relations for the element.

For incompressible solids, we introduce, instead of (16), the modified functional

$$\bar{V}(\mathbf{u}) = \int_{v_0} \hat{W}(I_1, I_2)\,\mathrm{d}v - p^{N\alpha}u_{N\alpha} + h\int_{v_0}(I_3 - 1)\,\mathrm{d}v \tag{22}$$

wherein h plays the role of a Lagrange multiplier and is assumed to be uniform over the element. Similar procedures have been used in earlier work [15, 16, 18, 19]. From the condition that $u_{N\alpha}$ be such that $\bar{V}[\mathbf{u}(u_{N\alpha})]$ assumes a stationary value ($\partial \bar{V}/\partial u_{N\alpha} = 0$), we arrive at the following nonlinear stiffness relations for a finite element of an isotropic, incompressible, elastic solid of revolution:

$$2\pi \int_{A_0} \frac{\partial \tilde{W}(I_1, I_2)}{\partial u_{N\alpha}} r\,\mathrm{d}r\,\mathrm{d}z + 2\pi h \int_{A_0} \frac{\partial I_3}{\partial u_{N\alpha}} r\,\mathrm{d}r\,\mathrm{d}z = p^{N\alpha}. \tag{23}$$

Equation (23) represents a system of six nonlinear equations in the seven unknowns $h, u_{N\alpha}(N = 1, 2, 3; \alpha = 1, 2)$. The seventh equation which must be added to complete the system is the incompressibility condition $H(u_{N\alpha}) = 0$ given in (20).

5. SPECIAL FORMS OF THE STIFFNESS RELATIONS

Specific forms of (23) can be obtained once the form of $\tilde{W}(\ )$ appropriate for the particular material under consideration is introduced. The well-known Mooney form of the strain–energy function,

$$\tilde{W}(I_1, I_2) = C_1(I_1 - 3) + C_2(I_2 - 3) \tag{24}$$

where C_1 and C_2 are constants, is often assumed in problems of finite elasticity, and the neo-Hookean form

$$\hat{W}(I_1) = C(I_1 - 3) \tag{25}$$

is particularly simple.

The nonlinear stiffness relations for a finite element of Mooney material are obtained by introducing (5), (15) and (24) into (23):

$$p^{N\alpha} = 2v_0 C_1 \frac{\partial \gamma_\beta^\beta}{\partial u_{N\alpha}} + v_0 C_2 \frac{\partial \varphi}{\partial u_{N\alpha}} + [C_1 + 2C_2(1 + \gamma_\beta^\beta)] \int_{v_0} \frac{\partial \lambda^2}{\partial u_{N\alpha}} dv_0$$

$$+ \int_{v_0} \left[2C_2 \frac{\partial \gamma_\beta^\beta}{\partial u_{N\alpha}} \lambda^2 + h \left(\lambda^2 \frac{\partial \varphi}{\partial u_{N\alpha}} + \varphi \frac{\partial \lambda^2}{\partial u_{N\alpha}} \right) \right] dv_0 \tag{26}$$

where v_0 is the undeformed volume of the element and

$$\left. \begin{aligned} \frac{\partial \gamma_\beta^\beta}{\partial u_{N\alpha}} &= b_\beta^N(\delta_\alpha^\beta + b_\beta^M u_{M\alpha}) \\[2mm] \frac{\partial \lambda^2}{\partial u_{N\alpha}} &= 2\frac{\lambda}{r} \delta_{1\alpha}(a^N + b_\beta^N x^\beta) \\[2mm] \frac{\partial \varphi}{\partial u_{N\alpha}} &= 2b_\lambda^N(\delta_\alpha^\beta + b_\beta^M u_{M\alpha})[\delta_\lambda^\beta + \gamma_{\rho\mu}(e^{\beta\rho} e^{\lambda\mu} + e^{\rho\lambda} e^{\mu\beta})] \end{aligned} \right\} \tag{27}$$

The nonlinear stiffness relations for a neo-Hookean material follow immediately from (26) by setting $C_2 = 0$.

A simplified form

The integration of terms in (26) which involve the circumferential extension ratio λ leads to extremely complicated logarithmic forms. To avoid these complications, we shall use instead of (15c) an approximate λ which is calculated using the average radial displacement over the element and which converges to the exact λ as the dimensions of the element are made arbitrarily small:

$$\lambda = 1 + \frac{\bar{u}_1}{\bar{r}} \tag{28}$$

Here $\bar{r}$ and $\bar{u}_1$ are the quantities defined in (21c, d). Then

$$\frac{\partial \lambda^2}{\partial u_{N\alpha}} = 2\frac{\lambda}{\bar{r}}(\delta^{N1} + \delta^{N2} + \delta^{N3})\delta^{\alpha 1} \tag{29}$$

and λ is treated as being uniform over the finite element. Equation (26) now reduces to the simplified form

$$p^{N\alpha} = 2v_0(C_1 + \lambda^2 C_2) \frac{\partial \gamma_\beta^\beta}{\partial u_{N\alpha}} + v_0[C_1 + 2C_2(1 + \gamma_\beta^\beta) + h\varphi] \frac{\partial \lambda^2}{\partial u_{N\alpha}} + v_0(C_2 + h\lambda^2) \frac{\partial \varphi}{\partial u_{N\alpha}}. \tag{30}$$

We remark once again that stiffness relations such as (30) represent six equations in the seven unknowns $h, u_{N\alpha}$ for each element. To these must be added an incompressibility condition (20) for each finite element.

Once the stiffness relations for a typical element are defined, the elements are assembled into an approximate connected model for the problem at hand. Since the process of assembling finite elements to form the discrete model is well-documented (e.g. [17], [18] or [29]), we shall not elaborate on it here. Suffice it to say that final equations involve element hydrostatic pressures and global values of the generalized nodal forces and displacements. Boundary conditions involve simply prescribing forces or displacements at boundary nodal points.

6. CHANGES IN LOADING

In the case of externally applied loads, the generalized forces $p^{N\alpha}$ of (18) are computed using the components of surface traction S^α referred to the coordinate lines in the undeformed body. The actual forces, however, are available to us only in the deformed body. Thus, the components S^α depend on the deformation, and it is necessary to express these forces in terms of the element deformations. In this section we derive general equations for the tractions S^α produced by an external pressure p and the corresponding forces $p^{N\alpha}$, which hold for arbitrary finite element approximations. Following a similar procedure, we then derive equations for the $p^{N\alpha}$ for triangular elements of revolution.

General

Consider an arbitrary solid body subjected to a uniform external pressure p. In the undeformed configuration C_0 we establish an intrinsic cartesian reference frame x^i which becomes curved in a deformed configuration C. An element of surface area dS_0 in the undeformed body with unit normal $\hat{n} = n_i i_i$ becomes dS in the deformed body, with unit normal $n = n^i G_i = n_i G^i$, where G_i, G^i are the natural base vectors in C. The cartesian coordinates of a point in the deformed body relative to the undeformed coordinates are denoted z_i. A two-dimensional view of the geometry is given in Fig. 2.

The total force exerted by the pressure on the element of area dS in the deformed body is given by

$$dF = -pn\, dS = -pn_i G^{ij} G_j\, dS \tag{31}$$

where G^{ij} is the contravariant metric tensor in the deformed body. Noting that

$$\sqrt{(G)}\hat{n}_i\, dS_0 = n_i\, dS \tag{32}$$

and

$$G_i = z_{j,i} i_j = (\delta_{ji} + u_{j,i})i_j \tag{33}$$

where u_j are the cartesian components of displacement and $G = |G_{ij}| = I_3$, we have

$$dF = -p\sqrt{(G)}\hat{n}_i(\delta_{jm} + u_{j,m})G^{im} i_j\, dS_0. \tag{34}$$

Thus, the components of surface force per unit undeformed area referred to the reference configuration are

$$S_j = -p\sqrt{(G)}\hat{n}_i(\delta_{jm} + u_{j,m})G^{im}. \tag{35}$$

In the case of symmetric, isochoric deformations of solids of revolution,

$$\left.\begin{array}{l} G^{\alpha\beta} = r^2\lambda^2(\delta^{\alpha\beta} + 2e^{\alpha\lambda}e^{\beta\mu}\gamma_{\lambda\mu}) \\ G^{\alpha 3} = 0, \qquad G^{33} = \varphi, \qquad G = 1 \end{array}\right\} \tag{36}$$
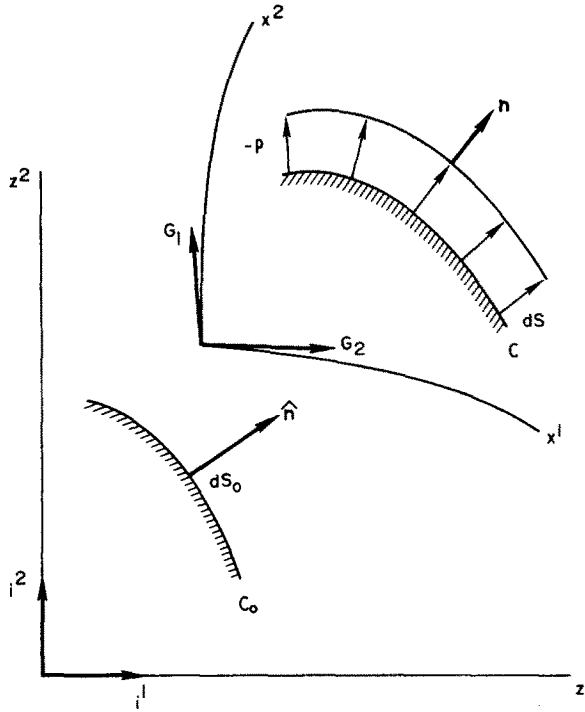
FIG. 2. Element of surface area in deformed and undeformed body.

and (35) becomes

$$S^\alpha = -pr^2\lambda^2\hat{n}_\lambda(\delta^\alpha_\mu + u^{\,\alpha}_{,\mu})(\delta^{\lambda\mu} + 2e^{\lambda\beta}e^{\mu\rho}\gamma_{\beta\rho}) \tag{37}$$

in which λ is given in terms of the radial component of displacement by (2).

Simplified forms

Equation (37) represents a quite complicated relation for the components of surface force. Fortunately, the forms of the final generalized nodal forces are significantly simplified if the boundaries are approximated by piecewise linear segments, as is the case in the present finite element model.

Consider the linear boundary of a triangular element of revolution, as shown in Fig. 3. The vector $\mathbf{L}$ connecting nodal points 1 and 2 in the deformed body is given by

$$\mathbf{L} = L_\alpha\mathbf{i}_\alpha = \mathbf{X}_2 - \mathbf{X}_1 \tag{38}$$

where

$$\mathbf{X}_1 = (x_{1\alpha} + u_{1\alpha})\mathbf{i}_\alpha \qquad \mathbf{X}_2 = (x_{2\alpha} + u_{2\alpha})\mathbf{i}_\alpha. \tag{39a, b}$$

Thus

$$L_1 = x_{21} - x_{11} + u_{21} - u_{11} \tag{40a}$$
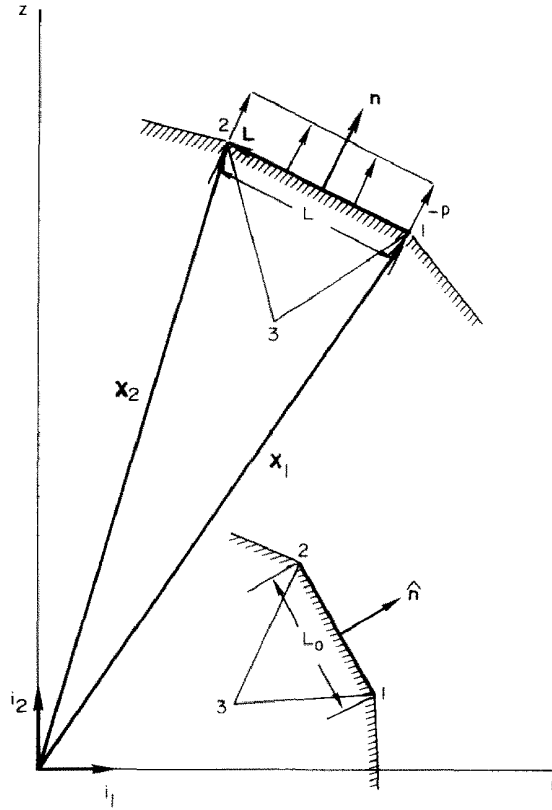
$$L_2 = x_{22} - x_{12} + u_{22} - u_{12} \tag{40b}$$

FIG. 3. Deformed and undeformed finite element boundaries.

and

$$L = |\mathbf{L}| = (L_1^2 + L_2^2)^{\frac{1}{2}} .$$

(41)

The total force developed on the boundary of the element is

$$\mathbf{F} = -p\pi(x_{21} + x_{11} + u_{11} + u_{21})L\mathbf{n}.$$

(42)

From the conditions

$$\mathbf{n} \cdot \mathbf{n} = 1 \qquad \mathbf{n} \cdot \mathbf{L} = 0$$

(43)

we find that

$$\mathbf{n} = \frac{1}{L} e^{\beta \alpha} L_\alpha \mathbf{i}_\beta .$$

(44)

Finally, distributing the total force $\mathbf{F}$ evenly between nodes 1 and 2 and introducing (44) into (42), we obtain for the components of the applied nodal forces

$$p^{1\alpha} = p^{2\alpha} = p\frac{\pi}{2}(x_{21} + x_{11} + u_{11} + u_{21})e^{\alpha\beta}L_\beta .$$

(45)

7. THE INFINITE CYLINDER PROBLEM

We now consider the special case of finite axisymmetric deformations of an infinitely long, thick-walled cylinder subjected to internal pressure. This problem is of special interest because (1) it is one of the few cases for which results can be compared with known exact solutions (cf. Green and Zerna [5]) and (2) it is one-dimensional, a fact which enables us to reduce the nonlinear stiffness relations to particularly simple forms. A more general two-dimensional problem is considered later.

The triangular finite elements of revolution developed previously can be used to portray axisymmetric (radial) deformations by constructing a finite-element model of a thin disk, as shown in Fig. 4a. Although the problem can be greatly simplified by equating the radial displacements of vertically opposed nodes I and I', the finite element characterization is subjected to a more severe test by allowing all nodes to displace freely in the radial direction. Then a model with E finite elements leads to $2E + 2$ nonlinear equations in the $E + 2$ unknown nodal displacements and E unknown element hydrostatic pressures.
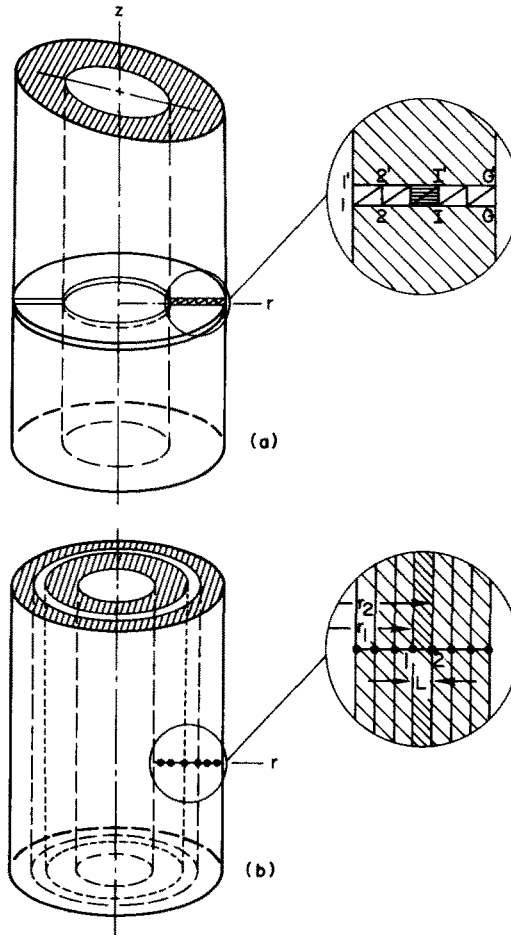

FIG. 4. Finite-element representations of an infinite cylinder.

As a first example a hollow cylinder, 7·00 in. internal radius and 18·265 in. external radius, of Mooney material with $C_1 = 80$ psi, $C_2 = 20$ psi is considered. The cylinder is subjected to an internal pressure of $p = 128·2$ psi. A cylinder with similar properties was examined by Baltrukonis and Vaishnav [10]. Displacement and hydrostatic pressure profiles for the case $E = 10$ (22 unknowns) are shown in Fig. 5. We see that for this rather crude representation slight differences occur between nodal values of radial displacement of vertically opposed nodes. For the ten-element case, these differences reach as much as 5 per cent, but the average values of top and bottom nodes differ from the exact by only 2 per cent. Hydrostatic pressures in the elements represent only rough averages for this coarse finite-element mesh. The values indicated in Fig. 5 are obtained by averaging the elemental hydrostatic pressures of adjacent (upper and lower) elements and assigning these values to points which are radially midway between nodes. The method of incremental loading, to be discussed subsequently, was used to solve the system of nonlinear equations generated in this example.

Element stresses, obtained by averaging the mean stresses in vertically adjacent elements, for the case of twenty elements are shown in Fig. 6. It is seen that very good agreement with the exact solution is obtained.
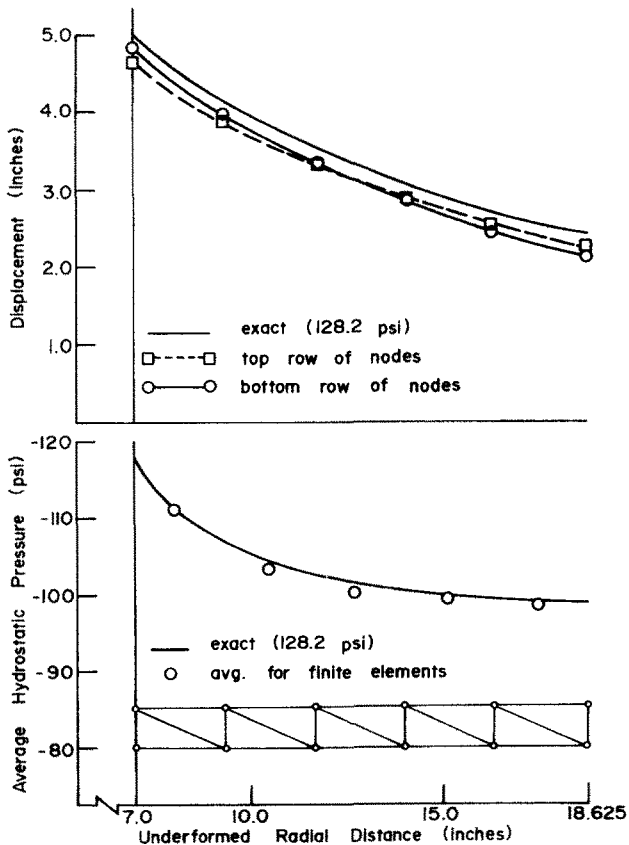

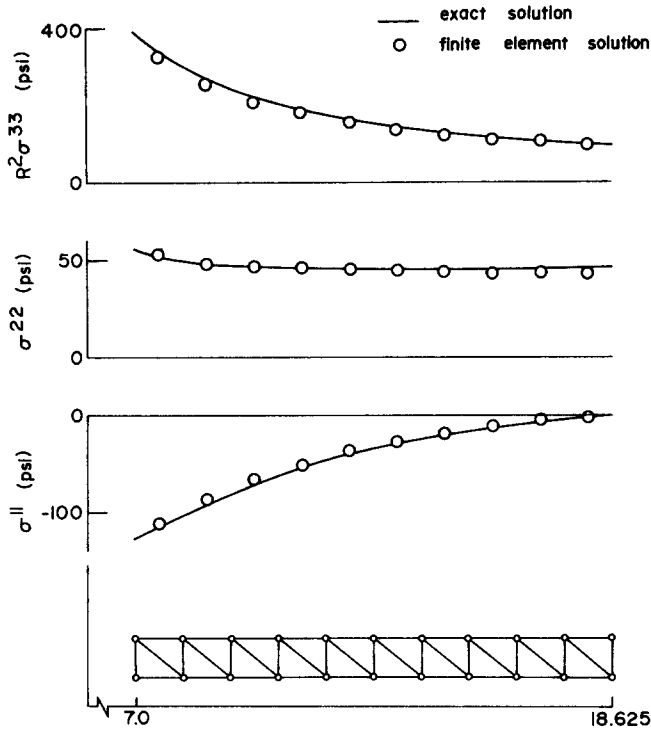FIG. 5. Displacement and hydrostatic pressure profiles.

FIG. 6. Stresses in cylinder.

Alternate representation

An alternate finite element representation of the infinite cylinder problem is obtained by using infinite, thin, cylindrical elements as indicated in Fig. 4b. Although numerical results obtained using this representation are practically the same as those obtained using models of the type in Fig. 4a, the stiffness equations derived from the purely one-dimensional kinematic relations are significantly simpler than those obtained from two-dimensional elements. Moreover, the slight discrepancies between displacements of vertically opposed nodes is automatically avoided.

For a one-dimensional element of unit height constructed of a Mooney material, we find that the nonlinear stiffness relations are

$$p^{N1} = 2\pi(r_2^2 - r_1^2)\left\{\frac{\Delta}{L}(e^{1N} + e^{2N})[C_1 + C_2(1+\lambda^2) + \lambda^2 h] + \frac{1}{2\bar{r}}\lambda[C_1 + C_2(1+\Delta^2) + \Delta^2 h]\right\} \quad (46)$$

where

$$\bar{r} = \tfrac{1}{2}(r_1 + r_2) \qquad L_0 = r_2 - r_1 \quad (47a, b)$$

and

$$\Delta = \frac{L}{L_0} = 1 + \frac{u_{21} - u_{11}}{L_0}, \qquad \lambda \approx 1 + \frac{u_{11} + u_{21}}{2\bar{r}}. \quad (48a, b)$$

The incompressibility condition is

$$1 = \lambda^2 \Delta^2 \tag{49}$$

and the generalized force at the interior (or exterior) node due to internal (external) pressure p is

$$p^{N1} = \pm\, 2\pi(r_N + u_{N1})p \tag{50}$$

where the positive or negative sign is used if p is an internal pressure (N is the interior node) or an external pressure (N is the exterior node), respectively.
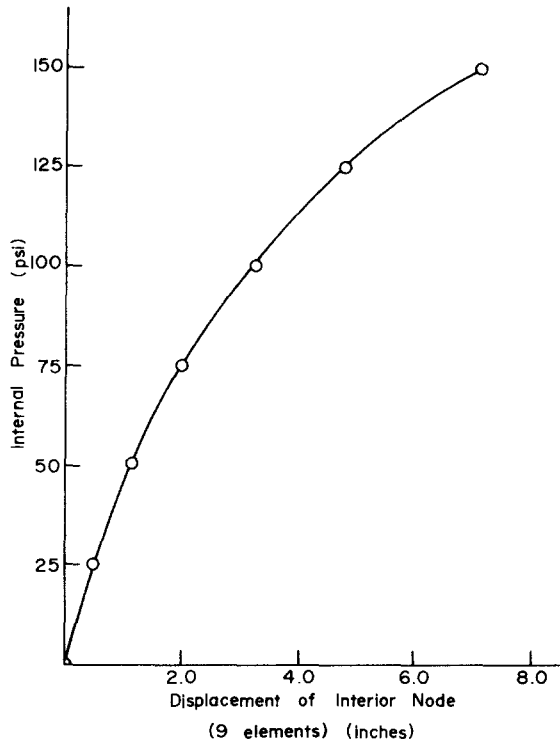

FIG. 7. Displacement of interior wall vs. internal pressure.

Some numerical results

Figures 7–11 contain numerical results obtained using (46)–(50) to solve the thick-walled cylinder problem described previously (i.e. $r_{int.} = 7\cdot00$ in., $r_{out.} = 18\cdot625$ in., $C_1 = 80$ psi, and $C_2 = 20$ psi). Solutions for a variety of internal pressures were obtained, ranging from 0 to 150 psi. For this material, an applied internal pressure of 150 psi corresponds to strains of the order of 150 per cent, so that the behavior falls well outside of that capable of being predicted by theory based on infinitesimal strains. For example, Fig. 7 indicates the variation of the displacement of the interior wall with the internal pressure, as computed using 9 finite elements. These results, which are indistinguishable from the exact solution, demonstrate that the behavior is decidedly nonlinear.
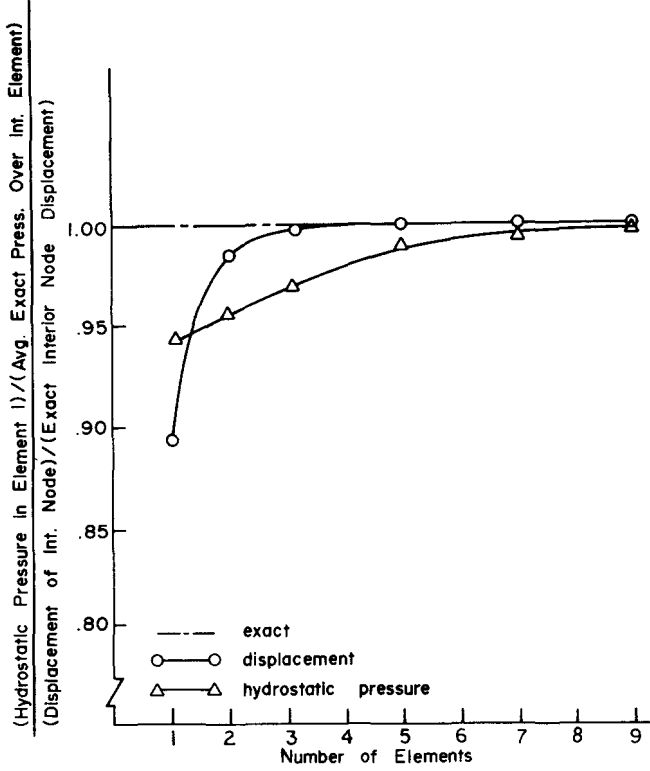
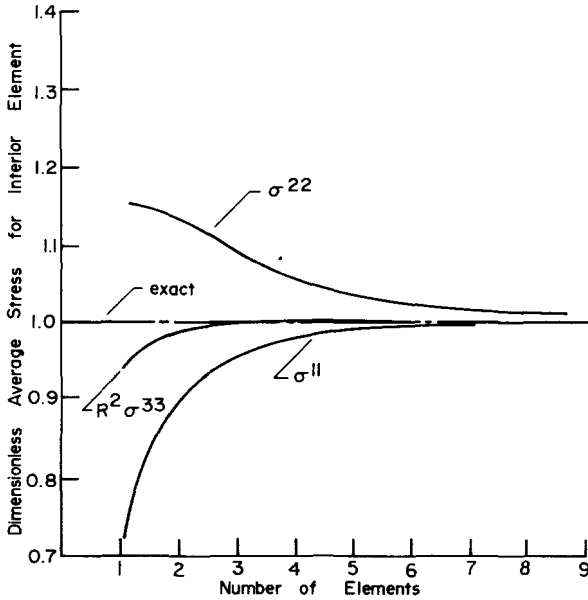FIG. 8. Convergence of finite-element solutions.

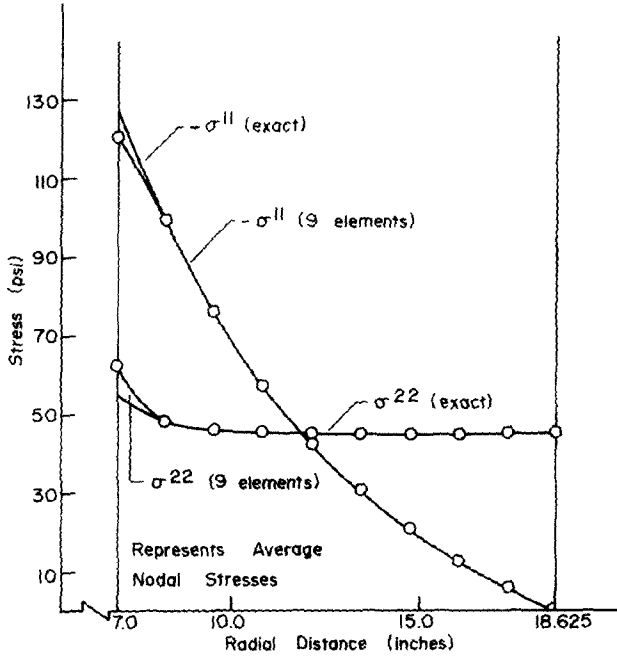FIG. 9. Convergence of average stress–interior element.
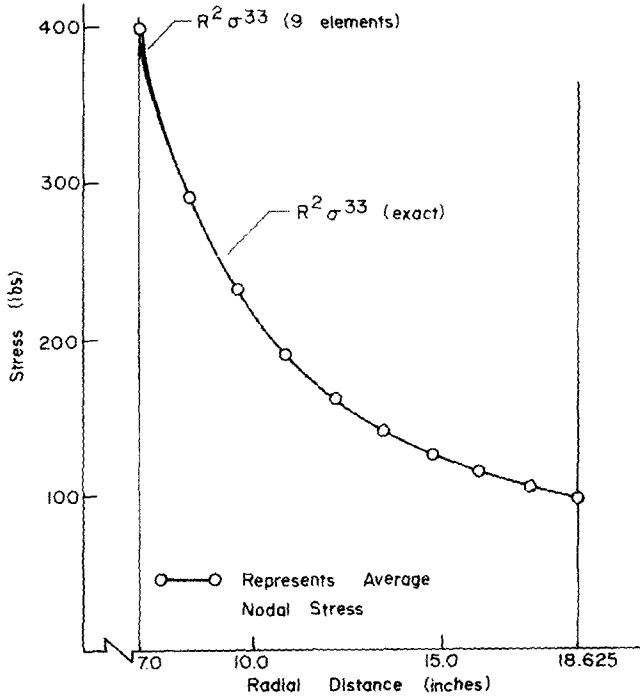
FIG. 10. Stress profiles—σ^{11} and σ^{22}.

FIG. 11. Stress profiles—$R^2\sigma^{33}$.

An indication of the convergence rate is given by Fig. 8. Here we see the ratios of the displacement of the interior wall to the exact displacement plus the ratio of the hydrostatic pressure in the first interior element to the average of the exact hydrostatic pressure over the element, plotted against the number of finite elements. Figure 9 shows the variation of the ratio of the average stress in this interior element to the exact average over the element versus the number of finite elements. We observe that convergence is not monotonic from below for all components, nor is it as rapid for all components as in the case of hydrostatic pressures. The stresses plotted in Figs. 10 and 11 represent averages of the predicted values of stress computed at each node. In the present finite element formulation, hydrostatic pressures are uniform over each element but actual stress components vary over the elements and the finite element solution exhibits a finite discontinuity in stress at each interelement boundary.

8. SOLUTION OF THE NONLINEAR EQUATIONS

In this section, we comment briefly on the numerical schemes used in solving the systems of nonlinear equations generated in the finite element analysis. The well-known Newton–Raphson method and the classical method of incremental loading were used to obtain all of the results presented in this paper. Attempts were also made to apply the Fletcher–Powell method [32] and the simplex search method [33] to the systems of nonlinear equations.

In general, we are interested in solving a system of N nonlinear equations which can be put in the form

$$f_i(x_1, x_2, \ldots, x_N) = p_i \qquad i = 1, 2, \ldots, N \tag{51}$$

where x_i are the unknowns (nodal displacements and hydrostatic pressures) and p_i represent prescribed nodal loadings. By introducing the column vectors $\mathbf{f}(\mathbf{x}) = \{f_1(\mathbf{x}), f_2(\mathbf{x}), \ldots, f_N(\mathbf{x})\}$, $\mathbf{x} = \{x_1, x_2, \ldots, x_N\}$, and $p = \{p_1, p_2, \ldots, p_N\}$, we can also write (51) in the form

$$\mathbf{f}(\mathbf{x}) = \mathbf{p} \tag{52}$$

The Newton–Raphson method

In the Newton–Raphson method, we expand $\mathbf{f}(\mathbf{x})$ in a Taylor series about a test point $\mathbf{x}^0$ and truncate to linear terms in the increment $\delta\mathbf{x} = \mathbf{x} - \mathbf{x}^0$:

$$\mathbf{p} = \mathbf{f}(\mathbf{x}^0 + \delta\mathbf{x}) \approx \mathbf{f}(\mathbf{x}^0) + \mathbf{J}(\mathbf{x}^0)\delta\mathbf{x}. \tag{53}$$

Here $\mathbf{J}(\mathbf{x})$ is the $N \times N$ jacobian matrix

$$\mathbf{J}(\mathbf{x}) = [\partial f_i(\mathbf{x})/\partial x_j]. \tag{54}$$

The solution $\mathbf{x}^n$ after n iterations is given by the recurrence formula

$$\mathbf{x}^n = \mathbf{x}^{n-1} - \mathbf{J}^{-1}(\mathbf{x}^{n-1})[\mathbf{p} - \mathbf{f}(\mathbf{x}^{n-1})]. \tag{55}$$

Although the Newton–Raphson method is one of the oldest techniques for solving nonlinear equations, it is one of the most reliable methods available. Among its obvious disadvantages are (1) an initial point (guess) $\mathbf{x}^0$ must be specified, (2) the inverse of $\mathbf{J}(\mathbf{x}^{n-1})$ must be computed for each cycle, (3) the functions $\mathbf{f}(\mathbf{x}^{n-1})$ and their gradients $[\partial f_i(\mathbf{x}^{n-1})/\partial x_j]$ must be evaluated each cycle and (4) without certain modifications, the method is

incapable of determining multiple solutions. On the other hand, it converges very quickly for the type of problem considered here; it is always possible to obtain estimates of error and of the rate of convergence, and, in principle, it can be extended so as to apply to systems of virtually any type of nonlinear equation, including systems of nonlinear differential and integral equations.

Incremental loading

The method of incremental loading is based on the idea that if the total load is applied in sufficiently small increments, the structure will respond linearly during each increment. In the present problem, nonlinear equations of the form

$$\mathbf{g}(\mathbf{x}, \mathbf{p}) = 0 \tag{56}$$

are obtained more naturally than the form indicated in (52). Then,

$$\delta\mathbf{g}(\mathbf{x}, \mathbf{p}) = 0 = \frac{\partial\mathbf{g}}{\partial\mathbf{x}}\delta\mathbf{x} + \frac{\partial\mathbf{g}}{\partial\mathbf{p}}\delta\mathbf{p} \tag{57}$$

and, instead of (55), we have

$$\mathbf{x}^n = \mathbf{x}^{n-1} - \mathbf{J}_p^{-1}(\mathbf{x}^{n-1}, \mathbf{p}^{n-1})\mathbf{G}(\mathbf{x}^{n-1}, \mathbf{p}^{n-1})\delta\mathbf{p}^n \tag{58}$$

wherein

$$\mathbf{J}_p(\mathbf{x}, \mathbf{p}) = [\partial g_i(\mathbf{x}, \mathbf{p})/\partial x_j] \tag{59}$$

$$\mathbf{p}^{n-1} = \sum_{i=1}^{n-1} \delta\mathbf{p}^i \tag{60}$$

$$\mathbf{G}(\mathbf{x}, \mathbf{p}) = \text{diag}[\partial g_i(\mathbf{x}, \mathbf{p})/\partial p_i]. \tag{61}$$

In applying the method of incremental loading, a given load $\mathbf{p}$ is broken into a number of increments $\delta\mathbf{p}$ and the procedure begins with zero displacements and hydrostatic pressures corresponding to zero load. The structure responds linearly to the first load increment. New structural properties, based on the deformed body after the first load increment, are computed and a second increment is applied. This process is repeated until all specified load increments are applied.

The method, though closely related to the Newton–Raphson method, is appealing on physical grounds. No initial "guesses" are required; the starting values have definite physical interpretations. Moreover, solutions to an entire family of problems are obtained in the solution process, and provisions for computing instabilities and multiple roots can be incorporated. Although new gradients $[\partial f_i/\partial x_j]$ must also be computed for each cycle, use of accurate finite difference approximations for these can be obtained without great difficulty. Such approximations can also be used in the Newton–Raphson method.

Accuracy of the solution obtained by the method of incremental loading depends upon the number of increments specified at the onset. Figure 12 shows the displacement of the interior node in the infinite cylinder problem vs. the internal pressure for 10, 20 and 40 load increments. For 40 increments, the displacement due to an internal pressure of 128·2 psi is 2·4 per cent in error, compared with an 8·8 per cent error for the 10 increment case. Although it is possible to improve solutions obtained by incremental loading by correcting the solution at the end of each cycle in a manner similar to the Newton–Raphson method, the small increase in accuracy afforded by such modifications was not deemed necessary in the present studies.
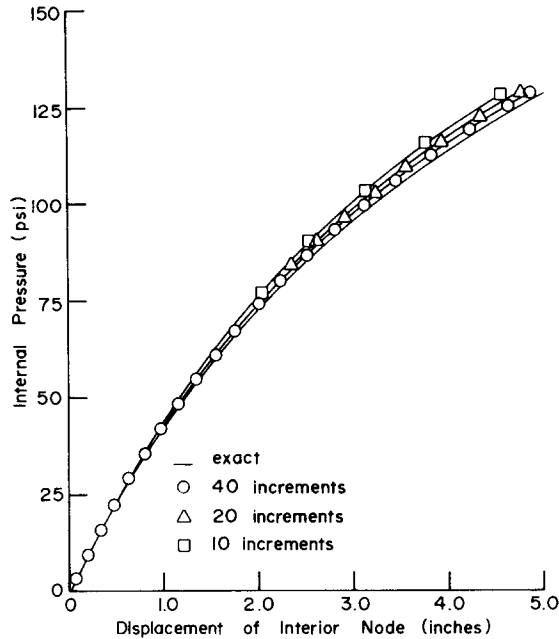
FIG. 12. Pressure–displacement curves obtained by incremental loading.

Other methods

Two well-known minimization methods were also used in an attempt to solve the nonlinear equations generated in this analysis. These are (1) the Fletcher–Powell method [32], a gradient technique based on quadratic convergence for functions of N variables and (2) the simplex-search method [33], a search routine that does not require the computation of a gradient. Details and comparisons of these methods can be found in [34]. For large systems of equations, the Fletcher–Powell method often converges faster than the Newton–Raphson method, but it may fail to converge in cases in which the Newton–Raphson method is successful [34]. The simplex search method is useful in cases in which regularity and continuity conditions present problems.

In the present analysis, an accuracy criteria was used wherein solutions obtained by a given method (FP, NR or simplex search) were required to differ no more than $\varepsilon = 0\cdot0001$ after 50 iterations. Neither the Fletcher–Powell nor the simplex search method were successful in any of the problems considered in this investigation.

9. INFLATION OF A THICK-WALLED CONTAINER

As a final example, we consider finite axisymmetric deformations of the thick-walled, incompressible elastic container shown in Fig. 13. Again, it is specified that the material be of the Mooney type [see equation (24)], with material constants $C_1 = 80\,\text{psi}$ and $C_2 = 20\,\text{psi}$. The body is subjected to a uniform internal pressure of 190 psi along the interior boundary BC. No forces are applied along AB.
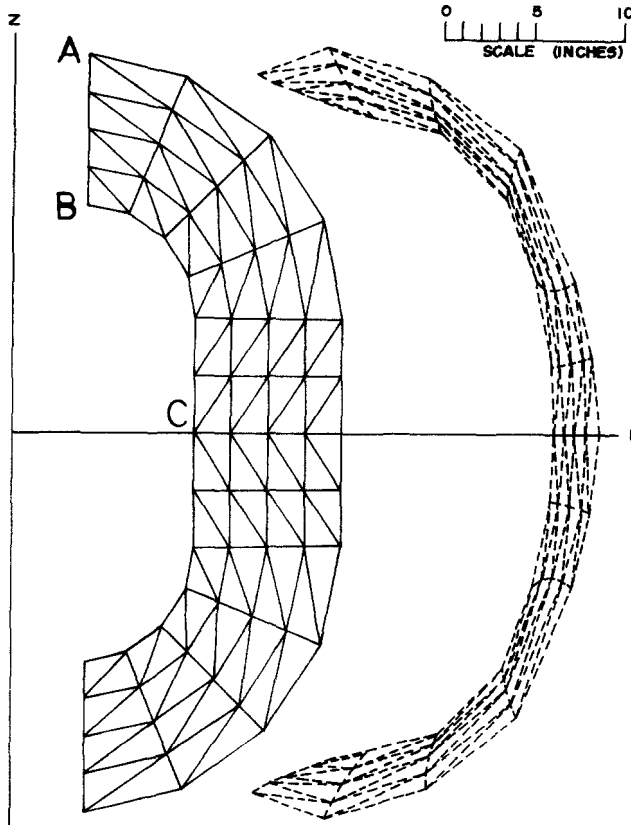
FIG. 13. Undeformed and deformed cross section of thick-walled highly elastic container subjected to internal pressure.

The finite-element representation for half of the container involves 48 finite elements connected together at 35 nodal points. This corresponds to 113 unknowns: 48 element hydrostatic pressures and 65 components of nodal displacement. The particular finite element model used in this analysis leads to nonlinear stiffness equations for each element which are polynomials of sixth-degree in the unknown nodal displacements and hydro-static pressures.

The method of incremental loading was used to solve the system of nonlinear equations, and nineteen 10 psi load increments were employed. Approximate gradients $[\partial f_i/\partial x_j]$, computed by finite differences with a specified $\Delta x_i = 0.0001$ were used in the recurrence formulas.

The deformed and unformed geometries of the assemblage of finite elements are shown to scale in the figure. Stress contours for components σ^{11} and $R^2\sigma^{33}$ shown in Fig. 14.
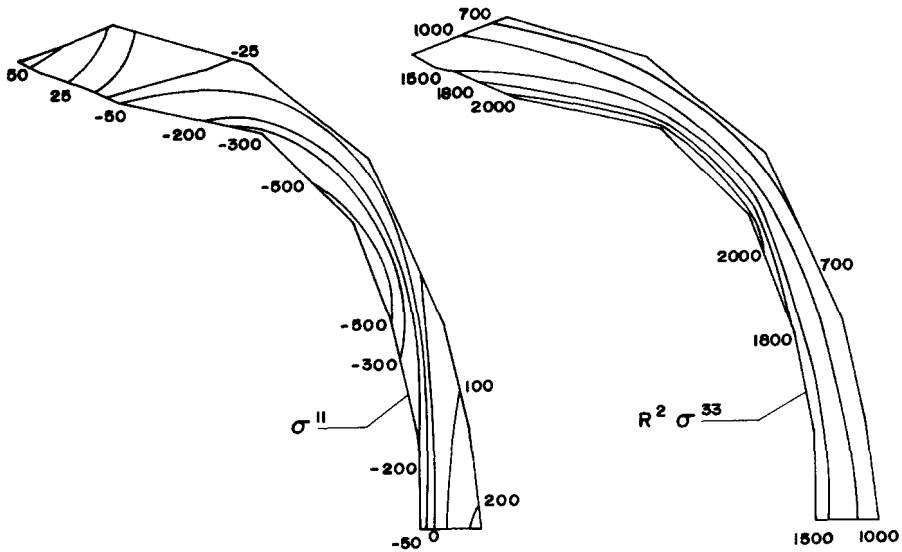
FIG. 14. Contours of radial stress $-\sigma^{11}$ and circumferential stress—$R^2\sigma^{33}$.

REFERENCES

[1] R. S. RIVLIN, Large elastic deformations of isotropic materials—VI. Further results in the theory of torsion, shear and flexure. *Phil. Trans. R. Soc.* **A242**, 173–195 (1949).

[2] J. L. ERICKSEN and R. S. RIVLIN, Large elastic deformations of homogeneous anisotropic materials. *J. rat. Mech. Analysis* **3**, 281–301 (1954).

[3] R. S. RIVLIN and A. G. THOMAS, Large elastic deformations of isotropic materials—VIII. Strain distribution around a hole in a sheet. *Phil. Trans. R. Soc.* **A243**, 289–298 (1951).

[4] A. E. GREEN and R. T. SHIELD, Finite extension and torsion of cylinders. *Phil. Trans. R. Soc.* **A244**, 47–86 (1951).

[5] A. E. GREEN and W. ZERNA, *Theoretical Elasticity*, 2nd edition. Clarendon Press (1968).

[6] A. E. GREEN and J. E. ADKINS, *Large Elastic Deformations and Non-Linear Continuum Mechanics*. Clarendon Press (1960).

[7] C. TRUESDELL and W. NOLL, The nonlinear field theories of mechanics. *Encyclopedia of Physics*, edited by S. FLÜGGE, Vol. III/3. Springer (1965).

[8] A. C. ERINGEN, *Nonlinear Theory of Continuous Media*. McGraw-Hill (1962).

[9] C. TRUESDELL (editor), *Continuum Mechanics—IV. Problems of Non-Linear Elasticity*. Gordon & Breach (1965).

[10] J. H. BALTRUKONIS and R. N. VAISHNAV, Finite deformations under pressurization in an infinitely long, thick-walled, elastic cylinder ideally bonded to a thin elastic case. *Trans. Soc. Rheol.* **9**, 273–291 (1965).

[11] Y. R. RASHID, Solution of elasto-static boundary value problems by the finite element method. Ph.D. Dissertation, University of California, Berkeley (1964).

[12] R. W. CLOUGH and Y. R. RASHID, Finite element analysis of axisymmetric solids. *J. Eng. Mech. Div., Am. Soc. civ. Engrs* **91**, 71–85 (1965).

[13] Y. R. RASHID, Analysis of axisymmetric composite structures by the finite element method. *Nucl. Engng Design* **3**, 163–182 (1966).

[14] E. L. WILSON, Structural analysis of axisymmetric solids. *AIAA Jnl* **3**, 2269–2274 (1965).

[15] E. B. BECKER and J. J. BRISBANE, Application of the finite element method to stress analysis of solid propellant rocket grains. Special Report No. S-76, Rohm & Haas Co., Huntsville, Alabama, November (1965).

[16] L. R. HERRMANN, Elasticity equations for incompressible and nearly incompressible materials by a variational theorem. *AIAA Jnl* **3**, 1896–1900 (1965).

[17] J. T. Oden, Analysis of large deformations of elastic membranes by the finite element method. *Proc. IASS Int. Congr. Large-Span Shells*. Leningrad, September (1966).

[18] J. T. Oden, Numerical formulation of nonlinear elasticity problems. *J. struct. Div. Am. Soc. civ. Engrs* **93**, 235–255 (1967).

[19] J. T. Oden, Finite plane strain of incompressible elastic solids by the finite element method. *Aeronaut. Q.* **19**, 254–264 (1968).

[20] J. T. Oden and T. Sato, Finite strains and displacements of elastic membranes by the finite element method. *Int. J. Solids Struct.* **3**, 471–488 (1967).

[21] J. T. Oden and T. Sato, Structural analysis of aerodynamic deceleration systems. *Adv. astro. Sci.* **24**, PS61–19 (1967).

[22] J. T. Oden and W. K. Kubitza, Numerical analysis of nonlinear pneumatic structures. *Proc. Int. Colloq. Pneumatic Structures*, Stuttgart, May (1967).

[23] E. Becker, A numerical solution of a class of problems of finite elastic deformations. Ph.D. Dissertation, University of California, Berkeley (1966).

[24] L. R. Herrmann, Nonlinear plane strain analysis applicable to solid propellant grains. *Bull. Fourth Meeting of the ICRPG Working Group on Mechanical Behavior*, Silver Spring, Md., November (1965), pp. 405–432.

[25] F. E. Peterson, D. M. Campbell and L. R. Herrmann, Nonlinear plane stress analysis applicable to solid propellant grains. *Bull. Fifth ICRPG Working Group on Mechanical Behavior*, Silver Spring, Md., November (1966), pp. 421–455.

[26] J. H. Argyris, Continua and discontinua. *Proc. Conf. Matrix Methods in Structural Mechanics*, Air Force Flight Dynamics Laboratory, TR-66-80, Wright-Patterson AFB, Dayton Ohio (1966), pp. 11–189.

[27] C. H. Parr, The application of numerical methods to the solution of structural integrity problems of solid propellant rockets—II. Solid Rocket Structural Integrity Information Center. *UTEC SI 67-001*, University of Utah, Salt Lake City, January (1967).

[28] J. T. Oden, A generalization of the finite element concept and its application to a class of problems in non-linear viscoelasticity. *Developments in Theoretical and Applied Mechanics*, Vol. 4. Pergamon Press (1968).

[29] J. T. Oden, A general theory of finite elements. *Int. J. Num. Method. Engng* **1**, 205–221 (1969).

[30] J. T. Oden, A general theory of finite elements—II. Applications. *Int. J. Num. Method. Engng* **1**, 247–259 (1969).

[31] J. T. Oden and G. Aguirre-Ramirez, Formulation of general discrete models of thermomechanical behavior of materials with memory. *Int. J. Solids Struct.* **5**, 1077–1093 (1969).

[32] R. Fletcher and M. J. D. Powell, A rapidly convergent descent method for minimization. *Comput. J.* **6**, 163–168 (1963).

[33] J. A. Nelder and R. Mead, A simplex method for function minimization. *Comput. J.* **7**, 308–313 (1965).

[34] K. L. Remmler, D. W. Cawood, J. A. Stanton and R. Hill, Solution of systems of nonlinear equations. Final Report, Lockheed Missile and Space Co./HREC, 0178-1, A783333, October (1966).

Абстракт—Работа обсуждает применение метода конечных элементов к задачам конечных, осесимметрических деформаций несжимаемых, упругих тел вращения. На основе приближенных полей деформаций, выводятся нелинейные зависимости для коэффициента жесткости типичного конечного злемента. Эти зависимости заключают член, обозначающий добавочное, неизвестное, гидростатическое давление, что требует введения условия несжимаемости для каждого элемента. Дается краткий обзор некоторых методов, используемых для решения систем нелинейных уравнений, обобщенных в предлагаемом анализе. Даются численные решения для иллюсмрации задач.